Environ. Sci. Technol. **2008,** *42,* 5828–5833

Removal of Oxide Nanoparticles in a Model Wastewater Treatment Plant: Influence of Agglomeration and Surfactants on Clearing Efficiency

LUDWIG K. LIMBACH,[†] ROBERT BEREITER,[‡,§] ELISABETH MÜLLER,[||] ROLF KREBS,[§] RENÉ GÄLLI,[‡] AND WENDELIN J. STARK*,[†]

Institute for Chemical and Bioengineering, Department of Chemistry and Applied Biosciences, ETH Zurich, CH-8093 Zurich, Switzerland, BMG Engineering AG, Ifangstrasse 11, CH-8952 Schlieren, Switzerland, Zurich University of Applied Sciences, Schloss, CH-8820 Wädenswil, Switzerland, and Electron Microscopy ETH Zurich (EMEZ), CH-8093 Zurich, Switzerland

Received January 10, 2008. Revised manuscript received May 14, 2008. Accepted May 15, 2008.

The rapidly increasing production of engineered nanoparticles has created a demand for particle removal from industrial and communal wastewater streams. Efficient removal is particularly important in view of increasing long-term persistence and evidence for considerable ecotoxicity of specific nanoparticles. The present work investigates the use of a model wastewater treatment plant for removal of oxide nanoparticles. While a majority of the nanoparticles could be captured through adhesion to clearing sludge, a significant fraction of the engineered nanoparticles escaped the wastewater plant's clearing system, and up to 6 wt % of the model compound cerium oxide was found in the exit stream of the model plant. Our study demonstrates a significant influence of surface charge and the addition of dispersion stabilizing surfactants as routinely used in the preparation of nanoparticle derived products. A detailed investigation on the agglomeration of oxide nanoparticles in wastewater streams revealed a high stabilization of the particles against clearance (adsorption on the bacteria from the sludge). This unexpected finding suggests a need to investigate nanoparticle clearance in more detail and demonstrates the complex interactions between dissolved species and the nanoparticles within the continuously changing environment of the clearing sludge.

Introduction

The rapid growth of nanotechnology has resulted in various implementations of nanomaterials in advantageous products or as process enhancers in manufacturing. As a result of the increasing production, it is important to obtain a better insight in possible risks related to these ultra small particles in the environment (*1*–*3*). Of particular interest is the clearing efficiency of nanomaterials within sewage plants that could avoid the propagation of nanoparticulate contamination into the aquatic environment. Possible toxic effects for aquatic species of insoluble carbon nanomaterials, such as carbon nanotubes, have been recently investigated on larval zebrafish (*4*) and *Daphnia magna* (*5*). Lovern et al. (*6, 7*) investigated acute toxicity and physiological changes of *D. magna* exposed to titania nanoparticles, one of the industrially most important metal oxides nanoparticles. These studies demonstrate a strong need to clarify possible entrances of nanoparticles into the aquatic environment.

However, little is known so far about the clearing efficiency of nanomaterials in sewage treatment. Reijnders (*8*) supposes that the standard wastewater treatment seems to be poorly suited to the capture of nanomaterials, whereas Wiesner et al. (*9*) did not support scenarios where containment of nanoparticles in current water treatment infrastructure may become problematic. Because of the present lack of experimental data, the disposal of nanomaterials is not regulated. This appears to be problematic because it is not clear what happens when inorganic nanomaterials are dispersed in the environment or brought into public sewage treatment plants.

The present work investigates the clearing of nanoparticles out of a model wastewater stream using a scalable model wastewater treatment according to guidelines of the Organization for Economic Co-operation and Development (OECD). As a model compound, we chose the industrially important cerium oxide which was already subject to numerous toxicological studies. These nanoparticles are used in the semiconductor manufacturing for chemomechanical polishing of silicon wafers (*10*) and polishing of lenses. Little is known about the influence and the behavior of cerium and other oxide nanoparticles on the environment. First indications can be taken from the existing few studies on the interactions of nanoparticles with organisms. The uptake of nanoparticles into a living cell was found to strongly depend on the material's agglomeration properties, making kinetic measurements rather challenging (*11*). Cytotoxic response of cerium and other oxide nanoparticles has been investigated for *Escherichia coli* (*12*), human lung cancer cells (*13*) and mesothelioma cells, and rodent fibroblasts (*14*). These studies suggest a complex behavior of nanoparticles in a wastewater treatment plant. A number of experimental studies (*11, 15, 16*) have shown that nanoparticles can change their behavior depending on the surrounding media in biological fluids, for example, through protein adsorption, implying that agglomeration, diffusion, and sedimentation of oxide particles change drastically if particles are brought into wastewater if compared to pure water (*11, 17*). Because most industrial applications of nanoparticles involve the use of surfactants, we investigated both pure oxide nanoparticle dispersions and stabilized formulations based on two industrially prominent surfactants.

The present investigation uses a setup according to OECD guidelines for the testing of chemicals (*18*). Originally, this setup was proposed to determine the elimination and the biodegradation of water-soluble organic compounds by aerobic microorganisms, (*19*) but it allows us to investigate the behavior of a broad range of materials in sewage treatment plants. This approach allows comparison of the present data to existing data sets of chemical compounds.

Experimental Section

General Experimental Design. After detailed characterization (see Supporting Information), both pure and surfactant stabilized cerium oxide nanoparticle dispersions were fed

* Corresponding author phone: +41 44 632 09 80; fax: +41 44 633 10 83; e-mail: wendelin.stark@chem.ethz.ch.
[†] Institute for Chemical and Bioengineering.
[‡] BMG Engineering AG.
[§] Zurich University of Applied Sciences.
[||] Electron Microscopy ETH Zurich.

10.1021/es800091f CCC: $40.75

Published on Web 06/25/2008

into a pre-equilibrated model wastewater treatment plant constructed according to OECD guidelines. This laboratory-scale model is established for testing of chemicals (*20*) and was adapted within this study to investigate nanoparticle behavior during biological treatment in a sewage plant. Additional treatment steps commonly used in sewage plants were not investigated. The clearing sludge was taken from the wastewater treatment plant of the city of Zurich, Switzerland, and checked continuously for respiration rate (viability) during all experiments. Particles were dispersed with either a nondegradable acryl polymer surfactant (Dispex A40, Ciba Specialty Chemicals, Germany) or biodegradable dodecyl benzyl sulfonic acid (Maranil, Cognis, Germany). Particle behavior was first investigated in different media at different ionic strengths and pH values. Selected suspensions were fed continuously into the clearing unit with growing sludge consisting of an aeration chamber followed by a settling vessel (Supporting Information, Figure S1). The total cerium oxide concentration at the outlet was measured by an inductively coupled plasma-optical emission spectrometer (ICP-OES). A centrifugation step allowed the unagglomerated cerium oxide nanoparticles and larger, sludge-bound nanoparticles to be distinguished. At the end of an experiment, the total cerium concentration was measured in the remaining sludge to close the mass balance.

The material and methods discussion is presented in the Supporting Information.

Results and Discussion

Physical Nanoparticle Properties. With the broad range of now available nanoparticles, detailed characterization of materials in their form of application is a prerequisite to both toxicological and environmental studies (*14, 21–28*). All studies have shown a dominating effect of surface charge (ζ-potential) on the kinetics of agglomeration and, as a consequence, on the physical behavior of the nanomaterials (*11, 15, 29*). To offer comparable data and for consistence with earlier studies on particle uptake (*11, 30–32*), cytotoxicity (*5, 6, 12, 14, 33–36*), and formation of reactive oxygen species (*37, 38*), the here investigated material was prepared by flame spray synthesis (*39*) using chloride-free precursors (*40*) and consists of nearly spherical, crystalline nanoparticles of 20−50 nm diameter (Supporting Information, Figures S2 and S3).

Nanoparticle Dispersion Stability. The stability of the here investigated cerium oxide dispersions was tested both for increasing pH and ionic strength in the surrounding medium. The addition of surfactants stabilizes the cerium oxide dispersions in water from pH 3 to 12, while pure cerium oxide precipitated around its isoelectric point at pH 8 (Supporting Information, Figure S4). As expected from its amphiphilic behavior, the addition of surfactants resulted in an improved dispersion stability even under high ionic strength (Supporting Information, Figure S5) as encountered in wastewater. Both pH and salts are strongly altering the tendency of the oxide nanoparticle dispersion to agglomeration and are consistent with earlier investigations on fullerene nanocrystals (*41*) and titania (*42*). This agglomeration behavior stays in line with a technically most important effect during polymer synthesis using emulsion polymerization (*43*). This production method proceeds in the form of a diluted emulsion and results in micro to millimeter-sized polymer spheres. To isolate the final polymer, the initially formed charge-stabilized polymer spheres are destabilized through the addition of salt, and the resulting aggregates (latex) can be easily separated by sedimentation.

Model Sewage Clearing Plant. Treatment of chemically contaminated wastewater has strongly profited from the development of scale-up correlations for sewage treatment plants. The present study applies exactly the same procedure, experimental setup, and sludge from a large-scale plant (Werdhölzli, Zurich city, Switzerland) to provide a comparison of nanoparticles to existing data on chemicals. Prior to exposure to oxide nanoparticle dispersions, the sludge was stabilized following the OECD guidelines (*18*). The content of dissolved organics (see Supporting Information, Figure S6) in the initiation period clearly demonstrated a reasonable level of stabilization after 100 h. Nanoparticle concentrations in the ranges of 100−1000 ppm were not acutely toxic for the bacteria (see Supporting Information, Figure S7).

Particle Clearance Efficiency. Thoroughly characterized cerium oxide dispersions (100 ppm, Supporting Information, Figure S3−S5) were continuously fed into the central sludge container. Treated water leaving the setup was analyzed using two methods: (A) total cerium oxide content in the outflow and (B) cerium oxide present as particles of less than 200 nm hydrodynamic diameter. The discrimination was done by selective centrifugation (*11*) prior to analysis and allowed larger aggregates or nanoparticles bound to bacteria (see Figure 3) and unagglomerated particles or very small aggregates (agglomerates of few particles sticking together; hydrodynamic aggregate diameter <200 nm) to be distinguished. Corresponding calculations and definitions are given in the electronic Supporting Information (Supporting Information, eq 4).

After an initial stabilization period, the total cerium oxide content in the treated wastewater stayed at 2−5 ppm (Figure 1). To gain additional insight into technically important sewage waters containing industrial tensides, we optionally applied a sulfonic acid (dodecyl benzene sulfonic acid, BSA) or a polyelectrolyte (poly acrylic acid, AP) with the oxide nanoparticle feed. The time-dependent outflow of total cerium oxide showed a steep increase for the first few hours and later partially leveled off if no (left) or a nondegradable surfactant (poly acrylic acid) was used to stabilize the particles (middle). The addition of a stabilizing but biodegradable tenside (right) promoted a longer increase of cerium oxide content in the treated water. The influence of the surfactants and the prolonged stabilization potential of the biodegradable benzyl sulfonic acid (BSA, Figure 1c) is well visible for the small particle fraction (<200 nm, Figure 1f). The different profiles in Figure 1b and c can be explained on the basis of the different biodegradation of the polyelectrolyte (acrylate; not degradable) and the benzyl sulfonic acid (biodegradable). The sludge can adapt to the presence of benzyl sulfonic acid after about 50 h and starts digesting the benzyl sulfonic acid thus destabilizing the cerium oxide dispersion. As a consequence, less cerium oxide can leave the test unit (drop in cerium oxide between 50 and 100 h). The degradation of the benzyl sulfonic acid was experimentally confirmed by measuring the dissolved organic content (Supporting Information, Figure S6).

The pronounced differences in ceria concentrations before (top graphs, Figure 1a−c) and after centrifugation (bottom graphs, Figure 1d−f) shows that a significant portion of the ceria is present as large aggregates or bound to bacteria. The setup used here can not distinguish between large cerium oxide aggregates or bacteria-bound particles. As a consequence, electron microscopy investigations were carried out on the sludge itself (see below) which confirmed the presence of aggregated particles sticking to the bacteria (Figure 3). The considerable fluctuations in cerium concentration of out-flowing sludge reflect the dynamic structure and composition of a living sludge that continuously adapts to the wastewater composition. This also alters the affinity of cerium oxide nanoparticles to the bacteria surface and the degree of flock (large aggregates of bacteria) formation. As a result, the amount of nanoparticles in the outflow shows considerable variations (Figure 1a).

Stabilizing Effect of Wastewater. Ceria nanoparticles should strongly agglomerate at experimental conditions (pH

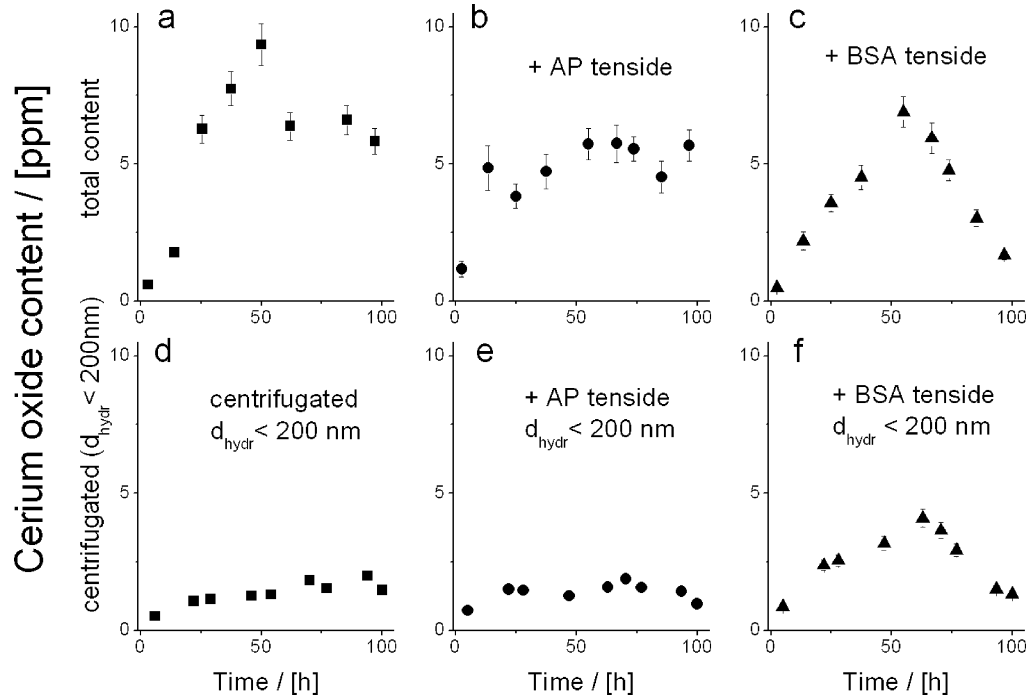

FIGURE 1. Oxide nanoparticle concentrations at the outlet of the activated sludge unit fed with model wastewater. Time-dependent concentration profile for pure cerium oxide (a), cerium oxide with an acrylic polymer surfactant, (b) and cerium oxide with an alkyl benzyl sulfonic acid surfactant (c). Small agglomerates and unagglomerated particles (d_{hydr} < 200 nm) were distinguished through an additional centrifugation step prior to analysis (d−f). Data represent individual runs. Error estimates are based on multiple measurements at a given time.

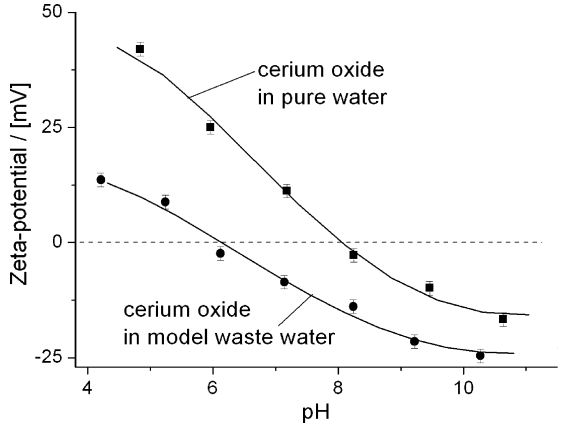

FIGURE 2. ζ-Potentials of 1 wt % cerium oxide dispersions in water and model wastewater as a function of acidity (pH). Dispersions are relatively stable for absolute ζ-potentials larger than 20 mV. The pronounced difference between wastewater and pure water is related to adsorption of stabilizing wastewater constituents, most probably peptides (see Supporting Information).

8−8.5) based on preliminary stability measurements (effect of salt addition and pH; see Supporting Information). To better understand the unexpected high level of unagglomerated cerium oxide in treated water (Figure 1; bottom series of graphs), a more detailed investigation on the ζ-potential of cerium oxide nanoparticles was made both in pure water and in model wastewater. The corresponding pH depending ζ-potential curve (Figure 2) is shifted through the constituents of wastewater by about 20 mV. The present findings on highly stabilized nanoparticle dispersions through model wastewater constituents (Figure 2) stays in agreement with earlier studies by Rezwan et al. (*44*) who demonstrated significant shifts in ζ-potential of colloids following adsorption of proteins. The study acts in further agreement with a study by Hyung et al. (*45*) that demonstrated carbon nanotubes stabilization by natural organic matter and with several studies on protein adsorption (*46–49*). To determine which component of the model wastewater contributed mostly to the shift, ζ-potential measurements of cerium oxide dispersions together with all single components of the wastewater were performed (Supporting Information, Figure S8). The largest contribution could be attributed to peptone, a component consisting of digested proteins, that is, small peptides. The adsorption of these peptides may therefore be linked to the enhanced stability of nanoparticles within the model wastewater.

While the particles rapidly agglomerate at neutral pH in water (low ζ-potential facilitates agglomeration), the constituents of wastewater significantly stabilize the dispersion, particularly at higher pH.

Nanoparticle Accumulation in the Sludge. Scanning transmission electron micrographs of sludge after contact to the cerium oxide dispersions showed aggregated nanoparticles together with the microorganism (Figure 3). The mass balance concerning cerium oxide inflow (100 ppm, total flow rate = 8.3 mL/min) and outflow (2−5 ppm, flow rate = 8.3 mL/min) could be closed within an error of 5% since we measured the nanoparticle accumulation in the sludge after the end of the experiments. The cerium oxide outlet concentration (Figure 1) was almost independent of the cerium oxide concentration in the perfectly mixed aeration chamber (Supporting Information, Figure S1) in spite of significant cerium oxide accumulation in the sludge over the time of an experiment (total duration = 100 h).

Residence Time Distribution. The residence time distribution of the model setup was measured in the aeration chamber and at the outlet performing a concentration step experiment (*50*) (Supporting Information, Figure S9). The residence time distribution supports the assumption of a continuously stirred tank reactor for the aeration chamber and a connected plug flow reactor for the settling vessel (Supporting Information, Figure S1). Both measured distributions are consistent with calculated ideal model reactors

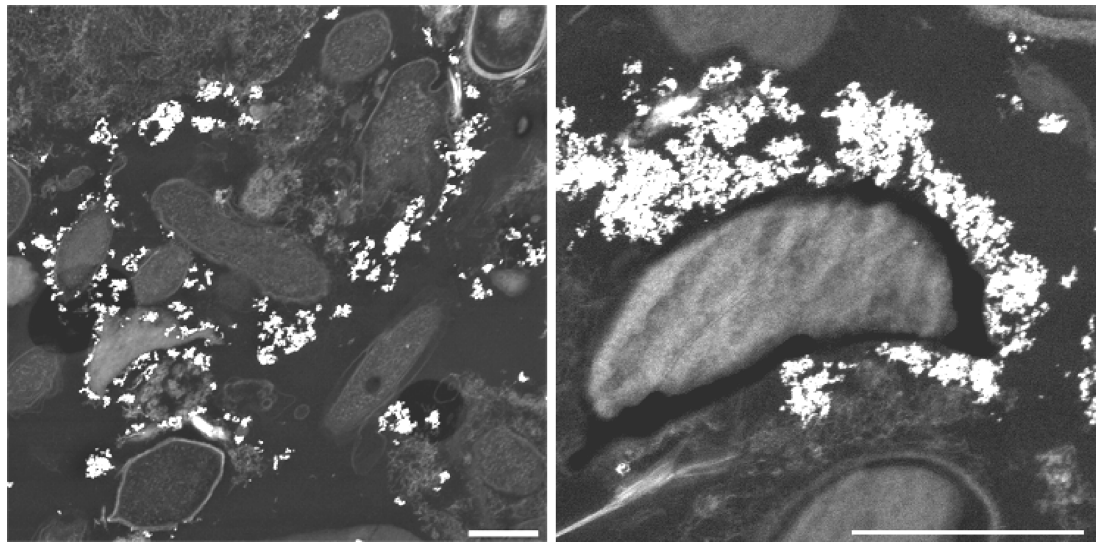

FIGURE 3. Scanning transmission electron micrograph of clearing sludge exposed to cerium oxide nanoparticles. In the Z-contrast images, the high density cerium oxide nanoparticles are bright. No particles were found within bacteria, but a cumulative appearance of cerium oxide around cells indicates preferred bonding to the sludge (bar size 500 nm).

known from chemical engineering (*50*). The medium residence time within the here used OECD setup was 8.03 h which is similar to the sewage water treatment plant of Zurich, Switzerland (ARA Werdholzli). Small, unagglomerated nanoparticles can leave the model plant because they sink slower than the water current moving through the unit from bottom to top. Larger agglomerates are retained in the unit because they continuously sink to the bottom of the unit and stay with the sludge. The critical aggregate radius could be calculated by balancing the sinking velocity to the upward fluid flow determined from the reactor geometry and residence time distribution. Depending on the fractal dimension and the density of the agglomerate, the critical aggregate radius was found to be 1−1.1 μm (see Supporting Information for definitions and details on the calculations). Because the majority of the aggregates observed by electron microscopy (Figure 3) were of smaller size, nanoparticles were predominantly cleared by adsorption to the sludge (bacteria). Because the bacteria are much larger and relatively heavy, such adsorbed particles stay in the unit and are removed from the wastewater. If only physical agglomeration of nanoparticles (no bacteria involved) were the dominating clearing step, much larger agglomerates would have to account for a considerably higher sinking speed.

Nanoparticle Breakthrough. Since earlier investigations (*11*) have demonstrated that oxide nanoparticle dispersions were relatively stable for ζ-potentials of at least 20 mV (absolute values; both positive or negative charge can be used to stabilize a dispersion), the observed high levels of cerium oxide (small fraction, < 200 nm) in the outflow must be a result from a low tendency of nanoparticles to agglomerate with the bacteria in the sludge. This is an unexpected finding because most oxide nanoparticle dispersions become instable if brought into the presence of high ion concentrations (Figure S5) or complex organic solutions (*11*). If the nanoparticles do not rapidly agglomerate and stick to the bacteria of the sludge, some of them are free to follow the water stream through the unit and eventually leave it.

This behavior is a direct result of the fact that the sludge is a living agglomerate of bacteria and subject to sludge agglomerate breakup, adhesion of sludge to gas bubbles, and occasional transfer of sludge into the outlet of the setup. To account for oxide nanoparticles that left the clearing unit in the form of adsorbed particles on sludge, a centrifugation step assured differentiation between bacteria bound nanoparticles (removable by the here chosen centrifugation step) and free (unbound) oxide nanoparticles. The location of oxide nanoparticles bound to the outer membrane of bacteria observed here was already observed by Thill et al. (*12*) during toxicity measurements of oxide nanoparticles. Electron microscopy combined with energy dispersive X-ray analysis on control experiments with or without cerium oxide confirmed the chemical identity and presence of the nanoparticles in the vicinity of bacteria (Figures S11 and S12).

Other Technically Important Oxide Nanoparticles. With the present rapid growth of novel products containing a range of different nanoparticles, we chose to further investigate the ζ-potential of some of the largest volume materials (*51*) in model wastewater (Figure 4). Similar to the behavior of nanoparticles in biological fluids (*11*), the individual nanoparticles showed very different surface charge if dispersed in pure water but displayed very similar ζ-potentials in model wastewater. This observation was consistent for all insoluble nanoparticle samples, while soluble (ZnO *14, 52*) or reactive (calcium-phosphates $Ca_3(PO_4)_2$ *14, 53, 54*) materials deviated from this trends (Figure 4, right), suggesting better particle clearance.

The later group (Fe_2O_3, ZnO, and $Ca_3(PO_4)_2$) represents materials that undergo chemical transformations (dissolution, recrystallization). As a result, protein and ion adsorption are expected to be different from the behavior of inert, nonreactive materials (left, Figure 4). Further investigations, however, will be required to elucidate the detailed behavior of a broader sample of nanoparticles in wastewater units.

The present study has taken a first step in the direction of investigating the clearing efficiency of sewage plants for oxide nanoparticles using a laboratory-scale model unit. Transfer of such findings to real-size plants can be subject to errors because of the scale up and must be critically reviewed. Additional experiments will be required for in-depth studies on the detailed mechanism of nanoparticle adsorption to sludge. The present results indicate a limited capability of the biological treatment step to completely remove oxide nanoparticles from wastewater. Separate investigations will be necessary to test the suitability of physical treatments (e.g., filtration) for improved oxide nanoparticle removal. The dominant role of agglomeration for nanoparticle mobility, diffusion, and even uptake into living cells is a physical characteristic depending on the square of the particle number concentration (*11*). The present study used an oxide nanoparticle concentration of 100 ppm mass

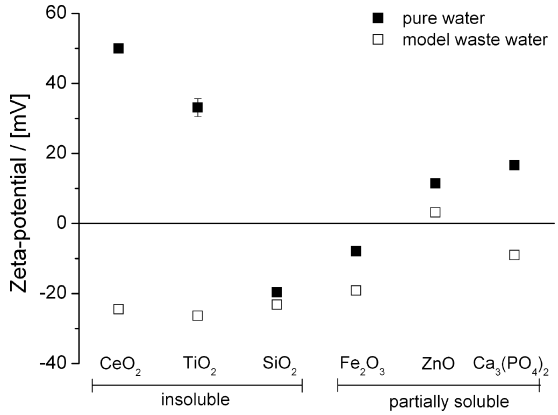

FIGURE 4. ζ-Potential measurements for different metal oxides and calcium phosphate nanoparticles in both water (filled symbols) and model wastewater (open symbols) showed a similar surface charge for insoluble materials, suggesting a similar clearance behavior of this group of materials. Slightly soluble or reactive nanoparticles (right) are less stable in wastewater and therefore expected to rapidly agglomerate and sediment during wastewater treatment.

(1.7×10^{12} particles/mL, 3.2 m^2 nanoparticle surface/L of liquid, or 1.3×10^{-5} cm^3 of oxide/mL of liquid). The lower concentrations expected in industrial wastewater disfavor agglomeration, and subsequently, particle removal through sedimentation. These findings motivate for detailed studies on the individual components of nanoparticles clearance, particularly in more dilute systems and eventually real-size plants. The high mobility of oxide nanoparticles in wastewater allows particles to spread over larger distances and makes monitoring of environmental distribution an analytically complex task.

Acknowledgments

We thank F. Krumeich for TEM analysis, L. Diener for preparation of the STEM samples, R. Wepf for cyro-SEM measurements, L. Gauckler for supporting ζ-potential measurements, N. Lederer for helpful discussions and the ARA Werdhölzli for supporting our investigations. Financial support by the Swiss Federal Office of Public Health (BAG, decision number 05.001872) is kindly acknowledged.

Supporting Information Available

Material and methods, supplementary results with detailed nanoparticle characterization and particle size measurements, full particle size distributions, and calculations on the sedimentation of particles in the test unit, details on the measurement of the residence time distribution of the setup and comparison to calculated flow profiles, combined with experimental data on sludge respiration rate and sludge toxicity of cerium oxide nanoparticles, and stability measurements of cerium oxide with constituents of wastewater and scanning electron micrographs of clearing sludge prior and after exposure to nanoparticles. This material is available free of charge via the Internet at http://pubs.acs.org.

Literature Cited

(1) Moore, M. N. Do nanoparticles present ecotoxicological risks for the health of the aquatic environment? *Environ. Int.* **2006**, *32*, 967–976.

(2) Owen, R.; Depledge, M. Nanotechnology and the environment: Risks and rewards. *Mar. Pollut. Bull.* **2005**, *50*, 609–612.

(3) Nowack, B.; Bucheli, T. D. Occurrence, behavior and effects of nanoparticles in the environment. *Environ. Pollut.* **2007**, *150*, 5–22.

(4) Cheng, J. P.; Flahaut, E.; Cheng, S. H. Effect of carbon nanotubes on developing zebrafish (*Danio rerio*) embryos. *Environ. Toxicol. Chem.* **2007**, *26*, 708–716.

(5) Roberts, A. P.; Mount, A. S.; Seda, B.; Souther, J.; Qiao, R.; Lin, S. J.; Ke, P. C.; Rao, A. M.; Klaine, S. J. In vivo biomodification of lipid-coated carbon nanotubes by *Daphnia magna*. *Environ. Sci. Technol.* **2007**, *41*, 3025–3029.

(6) Lovern, S. B.; Strickler, J. R.; Klaper, R. Behavioral and physiological changes in *Daphnia magna* when exposed to nanoparticle suspensions (titanium dioxide, nano-C-60, and C(60)HxC(70)Hx). *Environ. Sci. Technol.* **2007**, *41*, 4465–4470.

(7) Lovern, S. B.; Klaper, R. Daphnia magna mortality when exposed to titanium dioxide and fullerene (C-60) nanoparticles. *Environ. Toxicol. Chem.* **2006**, *25*, 1132–1137.

(8) Reijnders, L. Cleaner nanotechnology and hazard reduction of manufactured nanoparticles. *J. Clean Prod.* **2006**, *14*, 124–133.

(9) Wiesner, M. R.; Lowry, G. V.; Alvarez, P.; Dionysiou, D.; Biswas, P. Assessing the risks of manufactured nanomaterials. *Environ. Sci. Technol.* **2006**, *40*, 4336–4345.

(10) Jiang, M.; Komanduri, R. Chemical mechanical polishing (CMP) in magnetic float polishing (MFP) of advanced ceramic (silicon nitride) and glass (silicon dioxide). *Advances in Abrasive Processes*; Trans Tech Publications Ltd: Zurich-Uetikon, Switzerland, 2001; Vol. 202-2, pp 1−14.

(11) Limbach, L. K.; Li, Y. C.; Grass, R. N.; Brunner, T. J.; Hintermann, M. A.; Muller, M.; Gunther, D.; Stark, W. J. Oxide nanoparticle uptake in human lung fibroblasts: Effects of particle size, agglomeration, and diffusion at low concentrations. *Environ. Sci. Technol.* **2005**, *39*, 9370–9376.

(12) Thill, A.; Zeyons, O.; Spalla, O.; Chauvat, F.; Rose, J.; Auffan, M.; Flank, A. M. Cytotoxicity of CeO_2 nanoparticles for *Escherichia coli*. Physico-chemical insight of the cytotoxicity mechanism. *Environ. Sci. Technol.* **2006**, *40*, 6151–6156.

(13) Lin, W. S.; Huang, Y. W.; Zhou, X. D.; Ma, Y. F. Toxicity of cerium oxide nanoparticles in human lung cancer cells. *Int. J. Toxicol.* **2006**, *25*, 451–457.

(14) Brunner, T. J.; Wick, P.; Manser, P.; Spohn, P.; Grass, R. N.; Limbach, L. K.; Bruinink, A.; Stark, W. J. In vitro cytotoxicity of oxide nanoparticles: Comparison to asbestos, silica, and the effect of particle solubility. *Environ. Sci. Technol.* **2006**, *40*, 4374–4381.

(15) Rezwan, K.; Studart, A. R.; Voros, J.; Gauckler, L. J. Change of ξ potential of biocompatible colloidal oxide particles upon adsorption of bovine serum albumin and lysozyme. *J. Phys. Chem. B* **2005**, *109*, 14469–14474.

(16) Rezwan, K.; Meier, L. P.; Rezwan, M.; Voros, J.; Textor, M.; Gauckler, L. J. Bovine serum albumin adsorption onto colloidal Al_2O_3 particles: A new model based on ζ potential and UV−vis measurements. *Langmuir* **2004**, *20*, 10055–10061.

(17) Brant, J.; Lecoanet, H.; Wiesner, M. R. Aggregation and deposition characteristics of fullerene nanoparticles in aqueous systems. *J. Nanopart. Res.* **2005**, *7*, 545–553.

(18) Organization of the Economic Collaboration and Development. *Guideline for the testing of chemicals 303 A, Simulation Test - Aerobic Sewage Treatment Activated Sludge Unit*; OECD: Paris, 2001

(19) Junker, T.; Alexy, R.; Knacker, T.; Kummerer, K. Biodegradability of C-14-labeled antibiotics in a modified laboratory scale sewage treatment plant at environmentally relevant concentrations. *Environ. Sci. Technol.* **2006**, *40*, 318–324.

(20) Boeije, G.; Corstanje, R.; Rottiers, A.; Schowanek, D. Adaptation of the CAS test system and synthetic sewage for biological nutrient removal—Part I: Development of a new synthetic sewage. *Chemosphere* **1999**, *38*, 699–709.

(21) Borm, P.; Klaessig, F. C.; Landry, T. D.; Moudgil, B.; Pauluhn, J.; Thomas, K.; Trottier, R.; Wood, S. Research strategies for safety evaluation of nanomaterials, Part V: Role of dissolution in biological fate and effects of nanoscale particles. *Toxicol. Sci.* **2006**, *90*, 23–32.

(22) Oberdorster, G.; Oberdorster, E.; Oberdorster, J. Nanotoxicology: An emerging discipline evolving from studies of Ultrafine particles. *Environ. Health Perspect.* **2005**, *113*, 823–839.

(23) Powers, K. W.; Brown, S. C.; Krishna, V. B.; Wasdo, S. C.; Moudgil, B. M.; Roberts, S. M. Research strategies for safety evaluation of nanomaterials. Part.VI. Characterization of nanoscale particles for toxicological evaluation. *Toxicol. Sci.* **2006**, *90*, 296–303.

(24) Warheit, D. B.; Borm, P. J. A.; Hennes, C.; Lademann, J. Testing strategies to establish the safety of nanomaterials: Conclusions of an ECETOC workshop. *Inhal. Toxicol.* **2007**, *19*, 631–643.

(25) Warheit, D. B.; Hoke, R. A.; Finlay, C.; Donner, E. M.; Reed, K. L.; Sayes, C. M. Development of a base set of toxicity tests using Ultrafine TiO_2 particles as a component of nanoparticle risk management. *Toxicol. Lett.* **2007**, *171*, 99–110.

(26) Worle-Knirsch, J. M.; Pulskamp, K.; Krug, H. F. Oops they.did it again! Carbon nanotubes hoax scientists in viability assays. *Nano Lett.* **2006**, *6*, 1261–1268.
(27) Nel, A.; Xia, T.; Madler, L.; Li, N. Toxic potential of materials at the nanolevel. *Science* **2006**, *311*, 622–627.
(28) Donaldson, K.; Stone, V.; Tran, C. L.; Kreyling, W.; Borm, P. J. A. Nanotoxicology. *Occup. Environ. Med.* **2004**, *61*, 727–728.
(29) Teeguarden, J. G.; Hinderliter, P. M.; Orr, G.; Thrall, B. D.; Pounds, J. G. Particokinetics in vitro: Dosimetry considerations for in vitro nanoparticle toxicity assessments. *Toxicol. Sci.* **2007**, *95*, 300–312.
(30) Porter, A. E.; Gass, M.; Muller, K.; Skepper, J. N.; Midgley, P.; Welland, M. Visualizing the uptake of C-60 to the cytoplasm and nucleaus of human monocyte-derived macrophage cells using energy-filtered transmission electron microscopy and electron tomography. *Environ. Sci. Technol.* **2007**, *41*, 3012–3017.
(31) Suzuki, H.; Toyooka, T.; Ibuki, Y. Simple and easy method to evaluate uptake potential of nanoparticles in mammalian cells using a flow cytometric light scatter analysis. *Environ. Sci. Technol.* **2007**, *41*, 3018–3024.
(32) Rothen-Rutishauser, B. M.; Schurch, S.; Haenni, B.; Kapp, N.; Gehr, P. Interaction of fine particles and nanoparticles with red blood cells visualized with advanced microscopic techniques. *Environ. Sci. Technol.* **2006**, *40*, 4353–4359.
(33) Chang, J. S.; Chang, K. L. B.; Hwang, D. F.; Kong, Z. L. In vitro cytotoxicitiy of silica nanoparticles at high concentrations strongly depends on the metabolic activity type of the cell line. *Environ. Sci. Technol.* **2007**, *41*, 2064–2068.
(34) Worle-Knirsch, J. M.; Kern, K.; Schleh, C.; Adelhelm, C.; Feldmann, C.; Krug, H. F. Nanoparticulate vanadium oxide potentiated vanadium toxicity in.human lung cells. *Environ. Sci. Technol.* **2007**, *41*, 331–336.
(35) Dhawan, A.; Taurozzi, J. S.; Pandey, A. K.; Shan, W. Q.; Miller, S. M.; Hashsham, S. A.; Tarabara, V. V. Stable.colloidal dispersions of C-60 fullerenes in water: Evidence for genotoxicity. *Environ. Sci. Technol.* **2006**, *40*, 7394–7401.
(36) Auffan, M.; Decome, L.; Rose, J.; Orsiere, T.; De.Meo, M.; Briois, V.; Chaneac, C.; Olivi, L.; Berge.Lefranc, J. L.; Botta, A.; Wiesner, M. R.; Bottero, J. Y. In vitro interactions between DMSA-coated maghemite nanoparticles and human fibroblasts: A physicochemical and cyto-genotoxical study. *Environ. Sci. Technol.* **2006**, *40*, 4367–4373.
(37) Long, T. C.; Saleh, N.; Tilton, R. D.; Lowry, G. V.; Veronesi, B. Titanium dioxide (P25) produces reactive oxygen species in immortalized brain microglia (BV2): Implications for nanoparticle neurotoxicity. *Environ. Sci. Technol.* **2006**, *40*, 4346–4352.
(38) Limbach, L. K.; Wick, P.; Manser, P.; Grass, R. N.; Bruinink, A.; Stark, W. J. Exposure to engineered nanoparticles to human lung epithelial cells: Influence of chemical composition and catalytic activity on oxidative stress. *Environ. Sci. Technol.* **2007**, *41*, 4158–4163.
(39) Madler, L.; Stark, W. J.; Pratsinis, S. E. Flame-made ceria nanoparticles. *J. Mater. Res.* **2002**, *17*, 1356–1362.
(40) Stark, W. J.; Madler, L.; Maciejewski, M.; Pratsinis, S. E.; Baiker, A. Flame synthesis of nanocrystalline ceria-zirconia: Effect of carrier liquid. *Chem. Commun.* **2003**, 588–589.
(41) Espinasse, B.; Hotze, E. M.; Wiesner, M. R. Transport and retention of colloidal aggregates of C-60 in porous media: Effects of organic macromolecules, ionic composition, and preparation method. *Environ. Sci. Technol.* **2007**, *41*, 7396–7402.
(42) Guzman, K. A. D.; Finnegan, M. P.; Banfield, J. F. Influence of surface potential on aggregation and transport of titania nanoparticles. *Environ. Sci. Technol.* **2006**, *40*, 7688–7693.
(43) Carpineti, M.; Ferri, F.; Giglio, M.; Paganini, E.; Perini, U. Salt-induced fast aggregation of polystyrene latex. *Phys. Rev. A* **1990**, *42*, 7347–7354.
(44) Rezwan, K.; Meier, L. P.; Gauckler, L. J. Lysozyme and bovine serum albumin adsorption on uncoated silica and AlOOH-coated silica particles: the influence of positively and negatively charged oxide surface coatings. *Biomaterials* **2005**, *26*, 4351–4357.
(45) Hyung, H.; Fortner, J. D.; Hughes, J. B.; Kim, J. H. Natural organic matter stabilizes carbon nanotubes in the aqueous phase. *Environ. Sci. Technol.* **2007**, *41*, 179–184.
(46) Lin, Y.; Allard, L. F.; Sun, Y. P. Protein.affinity of single-walled carbon nanotubes in water. *J.Phys. Chem. B* **2004**, *108*, 3760–3764.
(47) Denis, F. A.; Hanarp, P.; Sutherland, D. S.; Gold, J.; Mustin, C.; Rouxhet, P. G.; Dufrene, Y. F. Protein adsorption on model surfaces with controlled nanotopography and chemistry. *Langmuir* **2002**, *18*, 819–828.
(48) Gearheart, L. A.; Ploehn, H. J.; Murphy, C. J. Oligonucleotide adsorption to gold nanoparticles: A surface.enhanced raman spectroscopy study of intrinsically bent DNA. *J. Phys. Chem. B* **2001**, *105*, 12609–12615.
(49) Cedervall, T.; Lynch, I.; Lindman, S.; Berggard, T.; Thulin, E.; Nilsson, H.; Dawson, K. A.; Linse, S. Understanding the nanoparticle-protein corona using methods to quantify exchange rates and affinities of proteins for nanoparticles. *Proc. Natl. Acad. Sci. U. S. A.* **2007**, *104*, 2050–2055.
(50) Fogler, H. S. *Elements of Chemical Reaction Engineering*; Prentice Hall PTR: New York, 2001.
(51) Stark, W. J.; Pratsinis, S. E. Aerosol flame reactors for manufacture of nanoparticles. *Powder Technol.* **2002**, *126*, 103–108.
(52) Madler, L.; Stark, W. J.; Pratsinis, S. E. Rapid synthesis of stable ZnO quantum dots. *J. Appl. Phys.* **2002**, *92*, 6537–6540.
(53) Brunner, T. J.; Grass, R. N.; Bohner, M.; Stark, W. J. Effect of particle size, crystal phase, and crystallinity on the reactivity of tricalcium phosphate cements for bone reconstruction. *J. Mater. Chem.* **2007**, *17*, 4072–4078.
(54) Loher, S.; Stark, W. J.; Maciejewski, M.; Baiker, A.; Pratsinis, S. E.; Reichardt, D.; Maspero, F.; Krumeich, F.; Gunther, D. Fluoro-apatite and calcium phosphate nanoparticles by flame synthesis. *Chem. Mater.* **2005**, *17*, 36–42.

ES800091F